Skeletal Radiology (2019) 48:1525–1539
https://doi.org/10.1007/s00256-019-03204-1

REVIEW ARTICLE

Review article: the differential diagnosis of bone marrow edema on wrist MRI

WanYin Lim[1,2] · Asif Saifuddin[3,4]

Received: 5 December 2018 / Revised: 1 February 2019 / Accepted: 5 March 2019 / Published online: 22 March 2019

Abstract

There is a large variety of conditions that can result in 'bone marrow edema' or 'bone marrow lesions' (BML) in the wrist on magnetic resonance imaging (MRI). The combination of clinical history and the distribution of the BML can serve as a valuable clue to a specific diagnosis. This article illustrates the different patterns of BML in the wrist to serve as a useful guide when reviewing wrist MRI studies. Imaging artefacts will also be briefly covered.

Keywords MRI · Wrist · Marrow edema · Bone marrow lesion

Introduction

Bone marrow lesions (BML), or marrow signal hyperintensity on fluid-sensitive magnetic resonance imaging (MRI) sequences, are observed in up to 36% of patients undergoing wrist MRI [1]. With regard to definition, the term 'bone marrow lesion' (BML) used in this manuscript is synonymous with 'edema-like marrow signal', 'marrow edema-like signal' or 'bone marrow edema pattern' [2]. These are better known in classical teaching as 'marrow edema', a term first used in the 1980s [3]. Since there is little radiological-pathological correlation between 'marrow edema' identified on MRI with histological evidence of interstitial edema, with pathology samples often revealing a mixture of increased interstitial fluid, hemorrhage, lymphocytes, and vascularization as well as necrosis and fibrosis, there has been a shift away from the term 'marrow edema' [2, 4].

The etiology of BMLs can also be confusing due to the non-specific appearance, MRI demonstrating poorly defined reduced T1-weighted spin echo (T1W SE) marrow signal intensity (SI) (Fig. 1a) with corresponding hyperintensity on short tau inversion recovery (STIR), fat-suppressed T2W fast spin echo (FS T2W FSE), and fat-suppressed proton density-weighted fast spin echo (FS PDW FSE) sequences (Fig. 1b). There may also be overlapping patterns between different entities, but the combination of clinical history and lesion location may allow for a more specific diagnosis.

This review article provides a 'surgical sieve' mnemonic framework for assessing BMLs in the wrist, summarized as 'VITAMIN Cs & Ds'; vascular, infective, traumatic, autoimmune, metabolic, iatrogenic, and neoplastic. The two Cs stand for congenital and chronic regional pain syndrome (CRPS), while the Ds are for disuse and degenerative. This mnemonic works well for the adult wrist but not necessarily for the pediatric wrist, which is therefore considered separately. Lastly, potential artefacts mimicking BMLs will also be reviewed.

Vascular causes for BML

Avascular necrosis (AVN), as its name implies, is osteonecrosis due to the interruption of blood supply, the commonest location in the wrist being the scaphoid. This is due to the blood supply of the scaphoid being predominantly via the distal pole, and in the event of a scaphoid fracture, the blood supply to the proximal pole may be compromised [5, 6]. Osteonecrosis is also

✉ WanYin Lim
ynyn146@gmail.com

1 Dr Jones and Partners Medical Imaging, 226 Greenhill Road, Eastwood, SA 5063, Australia

2 Royal Adelaide Hospital, Port Rd, Adelaide, SA 5000, Australia

3 Royal National Orthopaedic Hospital, Brockley Hill, Stanmore HA7 4LP, UK

4 Everlight Radiology, Level 6 West, Euston Road, London NW1 3AX, UK

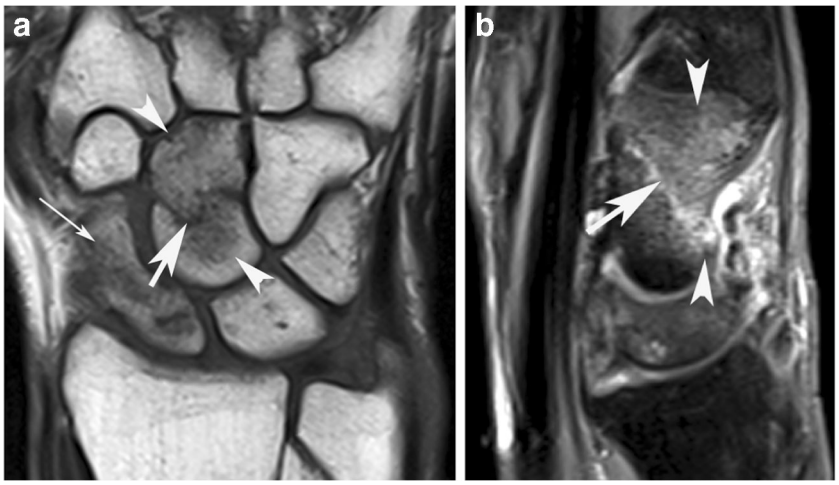

Fig. 1 MRI appearances of bone marrow lesions (BML). A 70-year-old female who fell on her outstretched hand. **a** Coronal T1-weighted spin echo (T1W SE) and **b** sagittal short tau inversion recovery (STIR) MR images showing an occult fracture of the capitate (*arrows*) associated with reduced bone marrow signal intensity (SI) on T1W and increased bone marrow SI on STIR due to a BML (*arrowheads*). BML is also noted in the scaphoid (*long arrow* in **a**) due to a trabecular injury

implicated in the etiology of various types of osteochondroses that involve the immature skeleton, such as Panner disease, Scheuermann's disease, Legg–Calve–Perthes disease, Sinding–Larsen–Johansson and Osgood–Schlatter disease, Kohler disease, and Sever disease [7]. However, none of these conditions involve the wrist or are associated with an acute traumatic event, and therefore the term AVN is preferred for post-traumatic scaphoid osteonecrosis.

MRI is an important technique for the investigation of radiographically occult scaphoid fractures [8]. BML may be seen in the early stages (Fig. 1), while in the late stages the devitalized bone tends to be sclerotic and returns T1W SE and STIR hypointensity (Fig. 2) [9]. It should also be noted that marrow hyperintensity on FS T2W FSE/STIR sequences does not necessarily indicate viable bone [10].

Preiser's disease represents idiopathic osteonecrosis of the scaphoid. Two types are described, type 1, where the whole bone is involved and type 2, where there is segmental osteonecrosis [11]. More recently, MRI has demonstrated three patterns of marrow abnormality [12] depending upon the degree and location of the necrosis. In the first stage, there is marrow abnormality limited to the proximal pole with normal scaphoid morphology (Fig. 3). In the second stage, there is associated pathological fracture in the zone of AVN associated with collapse, while in the final stage there is AVN of the whole bone. AVN can also produce a 'double-line' sign on T2W images comprising a hypointense line due to devitalized bone and a hyperintense line due to granulation tissue. This can be observed in the distal radius and ulna in the case of medullary infarction, although is rarely observed in carpal bones (Fig. 4) [13].

Kienbock's disease refers to AVN of the lunate [14–16]. The mechanism is multifactorial, including negative ulnar variance, which may compromise the vascular supply to the carpus. BML is one of the earliest signs (Fig. 5a, b), which in the presence of a normal radiograph equates to stage I of the Lichtman classification. This may be followed by sclerosis (stage II) and eventual collapse (stage IIIA), radiocarpal malalignment (stage IIIB) and secondary osteoarthritis (OA), which may result in a stress-related BML in adjacent bones (stage IV) (Fig. 5c, d) [15, 16].

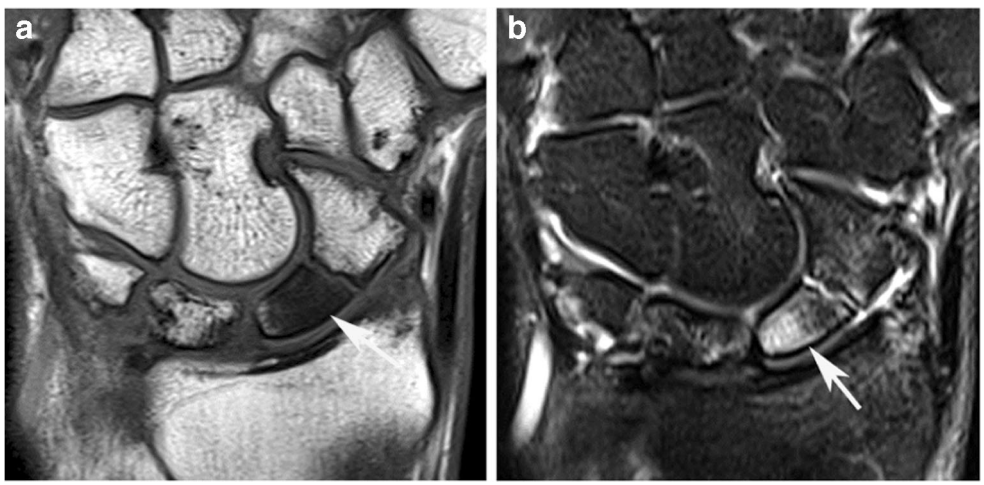

Fig. 2 Post-traumatic avascular necrosis (AVN) of the scaphoid. **a** Coronal T1W SE and **b** STIR MR images showing a scaphoid waist fracture with profound hypointensity in the proximal pole on T1W (*arrow* in **a**) consistent with AVN, and BML involving the proximal pole on STIR (*arrow* in **b**)

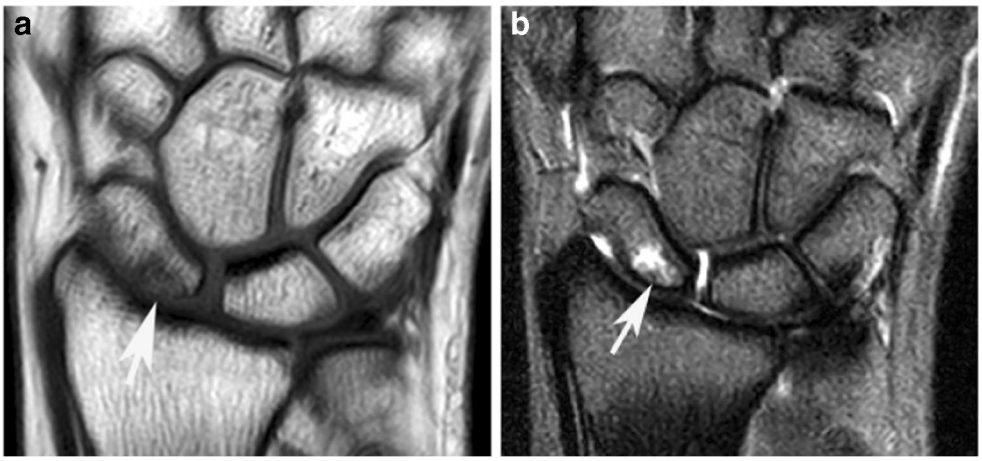

Fig. 3 Preiser's disease. A 29-year-old female with a previous history of femoral osteosarcoma and AVN of the right hip, who developed spontaneous wrist pain. **a** Coronal T1W TSE and **b** STIR MR images show a poorly defined BML in the proximal scaphoid (*arrows*) which was unchanged over 4 months, consistent with stage 1 Preiser's disease

AVN of the capitate has also been described, although rare [17].

Infective etiology

Osteomyelitis (OM) is associated with exuberant BML and can be an exudative or necrotic process. BML is secondary to hemorrhagic changes and congestion in exudative infection, while ischemia is implicated in necrotic infection [18]. In the hand and wrist, OM is usually due to direct inoculation, such as penetrating trauma and post-operative infection [19]. Tuberculous (TB) infection of the wrist can also produce osteomyelitis. Features suggestive of TB include synovial thickening around the flexor and extensor tendons, and tendon sheath effusions containing non-enhancing T2-weighted hypointense foci [20].

Fig. 4 Steroid-induced AVN of the scaphoid. Coronal STIR MR image of a 13-year-old boy with previous leukemia, showing a central medullary infarction within the scaphoid (*arrow*), and mild collapse of the proximal pole

Traumatic

Acute trauma

One of the major uses of wrist MRI is the assessment of occult fractures, particularly of the scaphoid [21, 22]. Scaphoid fractures represent approximately 70% of carpal fractures [23], and early MRI may potentially reduce the amount of time spent in a cast. In patients with clinically suspected scaphoid fractures but normal radiographs, MRI can be normal in 27% of cases, show a soft tissue injury in 43.4% of cases (Fig. 6), and show BML without a distinct fracture in 40.4% involving the scaphoid (Fig. 1a), other carpal bones (Fig. 1a, b) or the distal radius (Fig. 6), and a fracture in 22% [24]. The presence of scaphoid bone bruising alone is associated with the development of a fracture at 8 weeks follow-up in 2% of cases, with 92% of patients being asymptomatic by 8 weeks [25]. A hook of hamate fracture has also been reported in up to 10% of scaphoid fractures and can be associated with poor healing and chronic pain [26].

The mechanism of trauma usually determines the location and extent of BMLs. Compressive forces result in diffuse and poorly defined BML [4], as can be seen in the distal radius or ulna in patients presenting with a fall on the outstretched hand resulting in trabecular fracture (Fig. 7). Cortical or subchondral bone plate fractures may be seen, which are characterized by T1W or T2W hypointense lines associated with BMLs (Fig. 7a). If the BML has a broad-base abutting the subchondral bone plate, it is important to assess for overlying cartilage damage. The trabecular network has an intrinsic elastic property that is resistant to distraction. However, if the force is in excess of the elasticity, a linear BML ensues perpendicular to the vector of the stress [4]. If of sufficient magnitude, an avulsion fracture can occur as is typically seen from the dorsal surface of the triquetrum (Fig. 8), such fractures commonly associated with injury to the dorsal carpal ligaments [27].

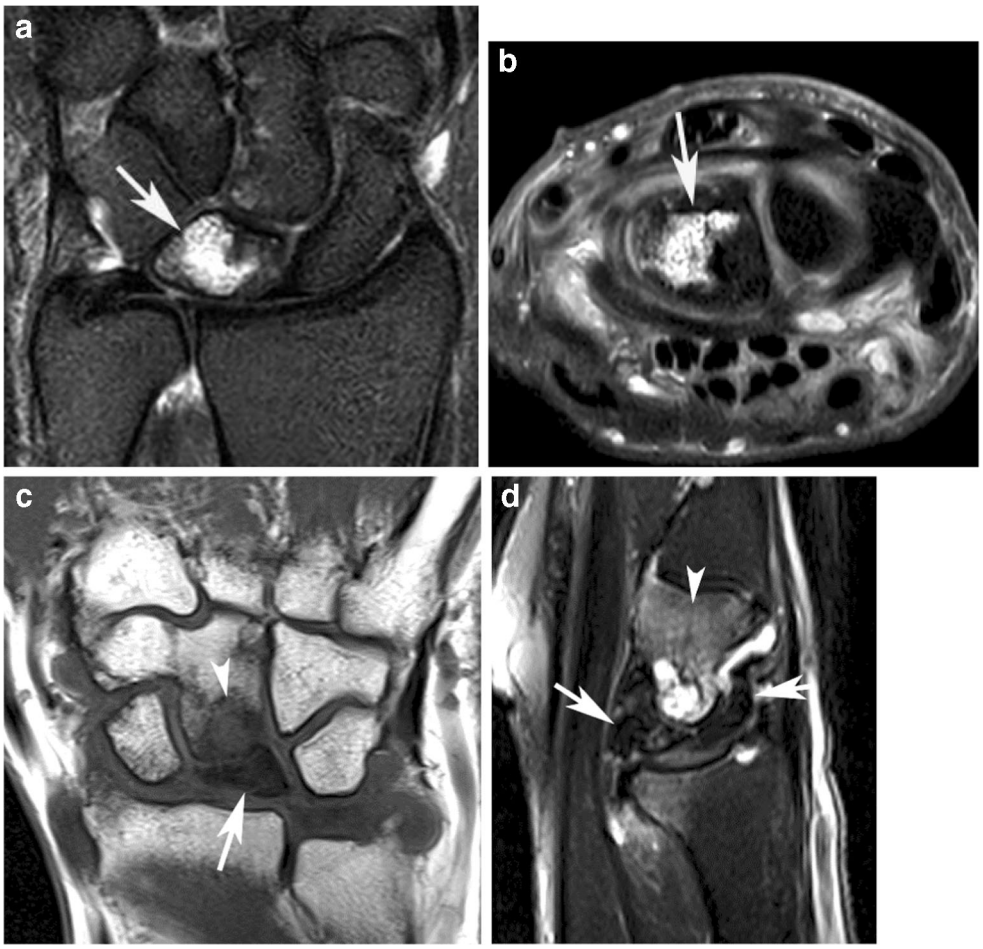

Fig. 5 Kienbock's disease. **a** Coronal STIR and **b** axial FS PDW FSE MR images of a 55-year-old male showing a BML involving the majority of the lunate (*arrow*), which otherwise appears intact, the features being consistent with stage I Kienbock's disease. **c** Coronal T1W SE and **d** sagittal STIR MR images of an elderly female with chronic wrist pain showing sclerosis, collapse, and fragmentation of the lunate (*arrows*), and subchondral cysts and BML in the capitate (*arrowheads*) due to mid-carpal OA consistent with stage IV Kienbock's disease

Chronic or non-acute injury

Stress fractures can be divided into fatigue or insufficiency types. Fatigue fractures are caused by repetitive stress or abnormal forces on normal bone, and in the wrist can be observed in the hook of hamate in climbers or with club and racquet sports [28, 29]. Gymnast wrist is another chronic overuse injury involving the distal radius [30], while stress injury of the lunate has also been described in elite tennis players, the BML usually involving the distal portion of the lunate [31]. In low-grade stress response, there is periosteal edema or cortical thickening, which may not be readily apparent. This is followed by BML, which can be sub-chondral or endosteal in location, usually wedge-shaped with its base

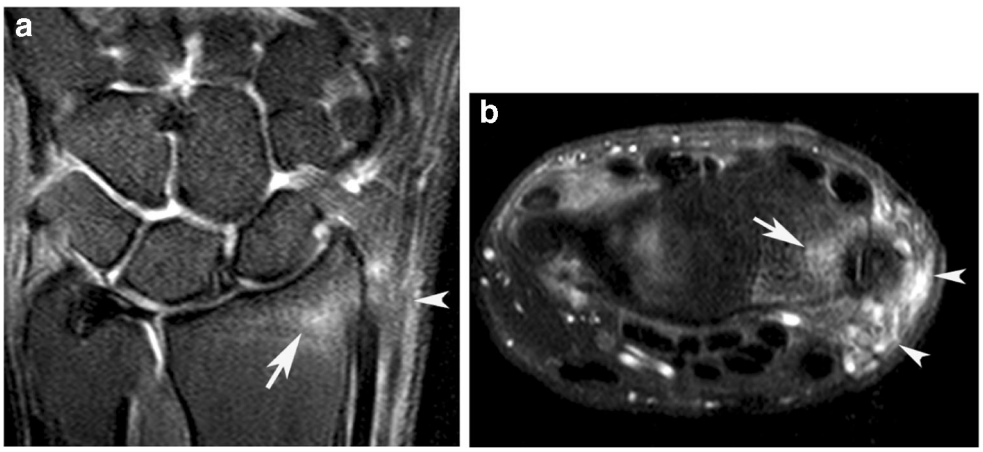

Fig. 6 Acute trauma. A 60-year-old female who fell on her hand. **a** Coronal and **b** axial STIR MR images showing mild bone bruising in the base of the radial styloid (*arrows*) and edema and swelling of the overlying soft tissues (*arrowheads*)

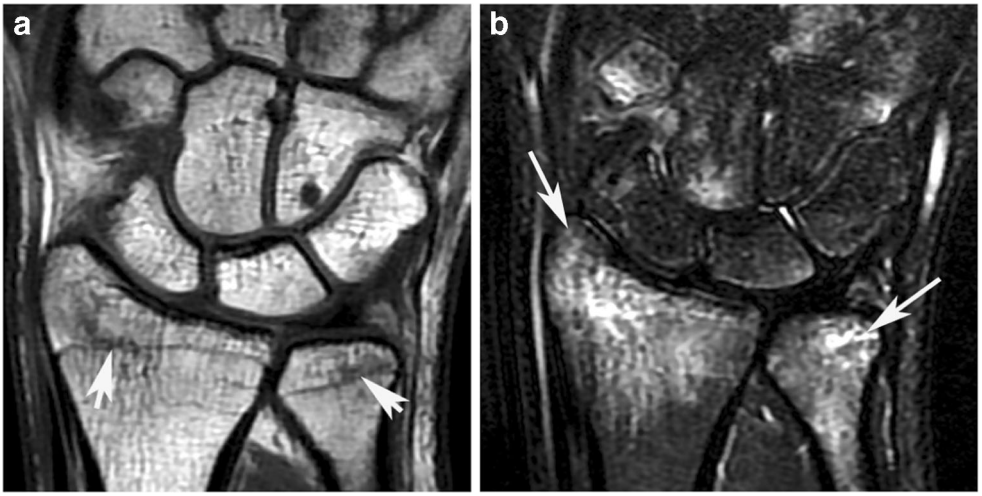

Fig. 7 Acute trauma. A 17-year-old male who fell on his hand. **a** Coronal T1W SE and **b** STIR MR images showing irregular hypointense lines in the distal radius and ulna due to occult fractures (*arrows* in **a**) and diffuse BMLs in the distal radius and ulna (*arrows* in **b**)

towards the site of the greatest stress [18]. In high-grade stress injuries, there will be corresponding T1W hypointensity in the region of the BML which can eventually be complicated by fracture.

Insufficiency fractures are caused by normal forces being applied on weakened bones, as in the context of osteoporosis. A common site in the wrist is the distal forearm due to preferential bone resorption at this location [32]. It is important to differentiate insufficiency fractures from pathological fractures, the latter being associated with marrow infiltration, soft tissue mass, or cortical destruction [32].

Ligament injury

The wrist is stabilized by a combination of intrinsic and extrinsic ligaments, including the triangular fibrocartilage complex [33]. BML can be associated with acute ligament injuries at the site of bony attachments in the event of a distractive force, such as the scaphoid attachment of the dorsal component of the scapholunate ligament [34]. In the chronic setting, untreated scapholunate ligament injury can result in progressive widening and dissociation of the scapholunate articulation, and secondary instability of the wrist, resulting in osteoarthritis (scapholunate advanced collapse/SLAC wrist) [35, 36]. The BML seen in this context will be secondary to chronic instability, centered at the radiocarpal articulation (stages I and II) (Fig. 9a) or at the mid-carpal joint (stage 3) (Fig. 9b). Similar features may be seen in scaphoid non-union advanced collapse (SNAC wrist) (Fig. 9c, d) [35].

There is also a high prevalence of extrinsic ligament injury in the setting of acute wrist trauma. Taneja et al. identified such injuries in 75% of patients undergoing wrist MRI for trauma, most commonly involving the radiolunotriquetral

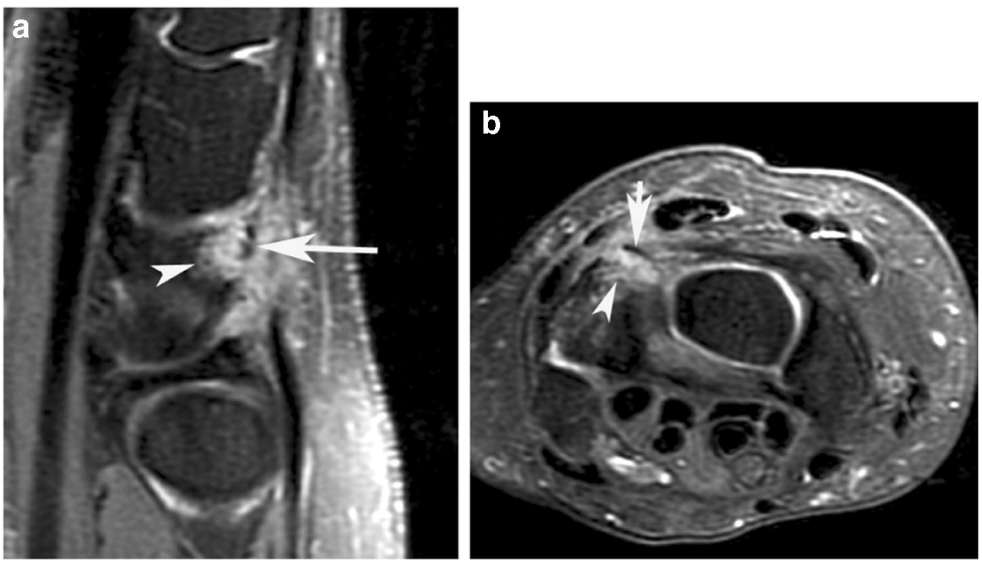

Fig. 8 Acute trauma. **a** Sagittal and **b** axial STIR MR images of a 51-year-old female showing a dorsal avulsion fracture of the triquetrum (*arrows*) with a mild associated BML (*arrowheads*)

Fig. 9 Scapholunate advanced collapse (SLAC wrist). **a** Coronal STIR MR image of a 53-year-old female showing mild widening of the scapholunate space and radioscaphoid OA consistent with stage II SLAC wrist, with BML in both bones (*arrows*). **b** Coronal STIR MR image of a 63-year-old male showing proximal migration of the capitate and mid-carpal OA consistent with stage III SLAC wrist, resulting in a BML in the capitate (*arrow*). A subchondral cyst with BML is also noted in the hamate (*arrowhead*). Scaphoid non-union advanced collapse (SNAC wrist). **c** Coronal T1W SE and **d** sagittal STIR MR images showing a non-united scaphoid waist fracture with proximal pole AVN (*arrow* in **c**), and OA between the distal pole and radial styloid (*arrowhead* in **c**) associated with a BML on both sides of the joint (*arrows* in **d**)

ligament. Extrinsic ligament injuries were significantly more common in association with bone abnormalities [37].

Mechanical causes for BML

A variety of impingement syndromes occuring around the wrist and are common causes of ulnar-sided wrist pain [23, 38]. Ulnar abutment syndrome (ulnocarpal impingement) is defined as chronic mechanical impaction between the ulnar head and the TFCC and lunate, resulting in a degenerative tear of the TFCC and chondromalacia of the proximal pole of the lunate and triquetrum [39]. This is associated with positive ulnar variance, which may follow an impaction fracture of the distal radius. In the early stages, BML can be observed in the distal ulna as well as proximal lunate (Fig. 10a) [40].

Ulnar impingement syndrome is due to shortening of the ulna, which impinges on the distal radial metaphysis on supination and pronation resulting in pain. BML can be seen at the site of the mechanical impingement (Fig. 10b) [40].

Ulnocarpal impaction syndrome results from a non-united ulnar styloid fracture [40]. When the fracture occurs through the base of the ulnar styloid (type 2 non-union), the ulnar attachment of the TFCC will be involved resulting in distal radioulnar joint (DRUJ) instability and possibly extensor carpi ulnaris (ECU) tenosynovitis. The non-united fracture fragment can result in chondromalacia of the proximal triquetrum with resulting BML.

Ulnar styloid impaction syndrome results from an elongated ulnar styloid (> 6 mm), which impacts on the adjacent triquetrum resulting in BML of the tip of the ulnar styloid and the proximal triquetrum (Fig. 10c, d). Chronic impaction may result in luno-triquetral instability and OA [40].

Hamato-lunate impaction syndrome arises due to impaction between the proximal pole of the hamate and a type 2 lunate, which has a separate distal articular facet. Recurrent impaction in ulnar deviation results in chondromalacia of the proximal pole of the hamate with an associated BML (Fig. 10e) [40].

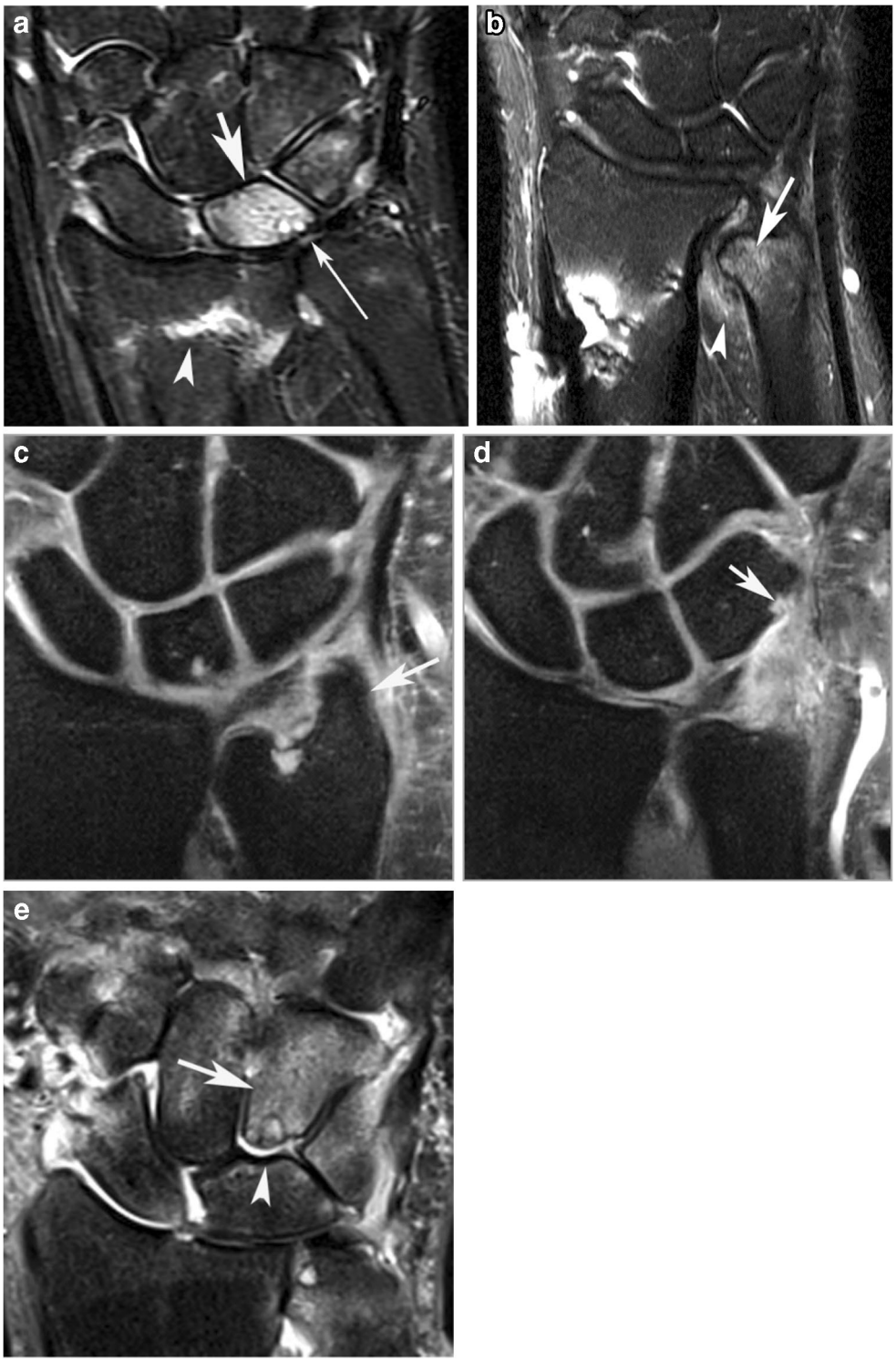

Fig. 10 Wrist impingement syndromes. **a** Ulnolunate abutment: Coronal STIR MR image of a 56-year-old female with positve ulnar variance due to an impacted distal radial fracture (*arrowhead*), associated with a degenerative tear of the TFCC disc (*thin arrow*) and prominent BML in the lunate (*arrow*). **b** Ulnar impingement: Coronal STIR MR image of a 34-year-old female with previous distal radial surgery and a short ulna which is impinging against the radial metaphysis resulting in BML in the ulnar head (*arrow*) and edematous swelling of the intervening soft tissues (*arrowhead*). **c** and **d** Ulnar styloid impingement: Coronal STIR MR images showing an elongated ulnar styloid (*arrow* in **c**), and a small BML in the triquetrum (*arrow* in **d**). **e** Hamato-lunate impaction syndrome: Coronal STIR MR image of a 76-year-old male showing a type 2 lunate morphology (*arrowhead*), hamato-lunate chondromalacia and an extensive BML in the hamate (*arrow*)

Autoimmune

Rheumatoid arthritis (RA) is a chronic multi-organ autoimmune disease which predominantly affects the skeletal system [41]. It is characterized by pain, stiffness, swelling, and reduced range of movement. Hyperplastic synovium induced by inflammatory mediators results in progressive cartilage damage, and erosions occur in most patients within a year of diagnosis. Treatment is aimed at reducing inflammation to minimize damage [42, 43].

BML is seen in 34–68% in RA, usually in the wrist (Fig. 11) [2]. Peri-articular BML observed in early and

Fig. 11 Rheumatoid arthritis (RA). **a** Coronal T1W SE and **b** STIR MR images of a 47-year-old female showing erosion of the ulnar styloid with associated BML (*arrow*) and widespread synovitis (*arrowheads*). **c** Axial T2W FSE MR image showing associated extensor tenosynovitis (*arrows*)

active RA is a sensitive and specific finding for inflammation, with good interobserver concordance [42–44], and also correlates with symptoms and severity. BML are associated with a sixfold increased risk of formation of erosions [2, 45], and BML in RA also appears to be associated with cartilage loss [46]. The value of MRI is in assessment of sub-clinical inflammation, which can alter therapy and outcome. BMLs have proven to be useful for risk stratification, prediction of clinical outcome, and monitoring of treatment response, particularly in the assessment of RA. To this effect, BML is now incorporated in Outcome Measures in Rheumatology Trials (OMERACT) and RAMRIS (Rheumatoid arthritis MRI study) for assessment of disease severity [47].

The sites of BML may aid differentiation of RA from other inflammatory arthropathies. In RA, changes are observed at sites of capsular attachment with intracapsular edema. Other spondyloarthropathies can produce extra-capsular edema in the acute phase. Psoriatic arthritis results in entheseal or ligamentous involvement and is associated with a higher risk of tenosynovitis. In this respect, there may also be BML at the insertion of the involved tendons [48].

BML in the wrist of patients with systemic lupus erythematosus (SLE) is similar to that in RA, but the hand is much less commonly involved in SLE [49].

Metabolic/endocrine

Although relatively uncommon in the wrist, crystal deposition in gout can occur at tendon insertions or along cartilage, and intraosseous extension of crystals can manifest as BML [50]. Synovitis, tophi, tenosynovitis and erosions can all be assessed on MRI and can be associated with BML [50]. BML can also be seen in the setting of acute gouty arthritis complicating chronic gout [51], but the presence of severe BML in patients with gout should raise the suspicion of associated osteomyelitis [52].

Iatrogenic

Post-operative

MRI may be needed following operation for various reasons, including ongoing pain. Depending upon the nature of the surgery, BML can be expected at the site of surgery for up to 12 months [18]. There may also be changes in the vascular supply or mechanics of the wrist post-operatively, which can contribute to the BML [18, 53].

Radiotherapy

The BML following radiotherapy can manifest within 1–14 days of radiotherapy and may last for anything from 3 weeks to several months following completion of treatment [18]. This can be associated with subcutaneous edema.

Neoplastic

BML can be observed in metastatic deposits due to the disruption of normal bone matrix, local inflammation or stress response, increasing the sensitivity of detecting lesions [18]. Primary tumors of the carpal bones are rare, with a reported prevalence of 0.16% [54]. The vast majority are benign (86%), the commonest being osteoid osteoma (25%) and the commonest locations being the scaphoid (30%) and capitate (22.7%) [54]. Osteoid osteoma may be radiographically occult, presenting only as exuberant reactive BML (Fig. 12a) [55]. Therefore, in the presence of a BML and clinical features suggestive of osteoid osteoma, a CT study may be required to demonstrate the nidus (Fig. 12b).

Another tumor that is typically associated with BML is chondroblastoma, a benign chondral lesion that frequently occurs in the epiphysis in young patients. Reactive synovitis is often present. The location and chondroid matrix may help distinguish this tumor from more aggressive lesions [56]. However, the wrist is a rare location for this tumor [57].

Complex regional pain syndrome (CRPS)

While this remains a clinical diagnosis, it is usually associated with a patchy BML pattern in the early phase, usually in a peri-articular sub-cortical distribution [58]. It can be distinguished radiologically from disuse osteopenia by the presence of skin edema and thickening.

Disuse osteopenia

Disuse osteopenia is commonly seen following immobilization, such as in cases of suspected scaphoid injury. It has a typical polka-dot BML morphology while other described patterns include patchy, sub-cortical (Fig. 13), sub-chondral bone plate, or sub-entheseal [59]. These are usually asymptomatic and can resolve within 18 weeks [60].

Degenerative

Wrist OA is usually secondary to trauma, metabolic arthropathy, or inflammatory conditions, with idiopathic wrist OA also occurring [61, 62]. Scapho-trapezio-trapezoidal OA (STT/triscape) has a reported radiographic prevalence of 59% in patients attending a specialist hand clinic, with radiocarpal OA evident in 29% of cases [63]. There is an association between BML and symptomatic OA in which BML is associated with progression of OA, and the extent of the BML is linked to

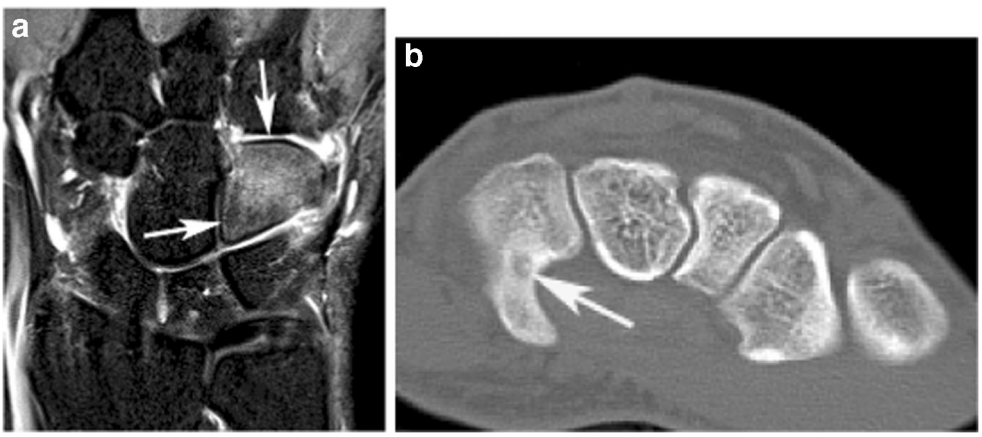

Fig. 12 Osteoid osteoma (OO). **a** Coronal STIR MR image of a 28-year-old male with chronic wrist pain showing a diffuse BML of the hamate (*arrows*). **b** Axial CT study demonstrates an OO nidus at the base of the hook of hamate (*arrow*)

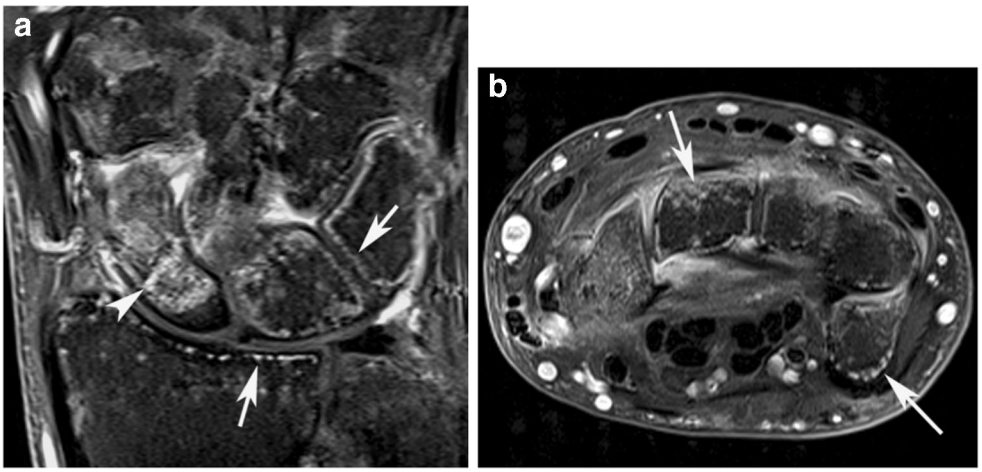

Fig. 13 Disuse osteopenia. **a** Coronal and **b** axial STIR MR images of a patients with an occult scaphoid waist fracture (*arrowhead* in **a**) showing widespread, predominantly subcortical BML (*arrows* in **a**, **b**)

the severity of cartilage loss [2, 18]. Subchondral cysts have been shown to develop in areas of BML [64] (Fig. 14). Ancillary imaging findings include chondral loss, osteophyte formation, joint effusion and synovitis.

The pediatric wrist

The diagnostic value of MRI in the pediatric population has been studied. Gornitzky et al. evaluated the impact of MRI in 307 consecutive children presenting to a tertiary care pediatric hospital [65]. The commonest indication was pain in which case MRI was normal in one-third of cases, while the greatest diagnostic impact was in the assessment of a mass/cyst, evaluation of infection and arthropathy. However, the authors concluded that MRI was not an ideal screening tool for children, particularly when the indication was pain and should only be used to confirm or exclude a specific diagnosis [65]. Conversely, Taylor et al. found that pediatric wrist MRI had a major impact, changing management in 86% of cases and altering diagnosis in 46% [66].

Fig. 14 Osteoarthritis (OA). Coronal STIR MR image of a 59-year-old male showing triscaphe OA (*arrow*) with associated BML in the scaphoid and trapezoid (*arrowheads*)

Normal variants

Foci of bone marrow hyperintensity may be seen on fluid-sensitive sequences in the distal forearm, carpal bones, and the bases of the metacarpals of asymptomatic children, these being commoner in younger children. They are thought to represent normal bone remodeling or residual red marrow [67]. Similarly, BML have been described in the wrists of approximately 40–50% of healthy children, and may persist over a period of up to 4 years. They are typically located in the central parts of the bone, on either side of a joint or near bony depressions. The scaphoid, capitate, and hamate were most commonly affected. Carpal effusions and ganglion cysts are also relatively common findings [68].

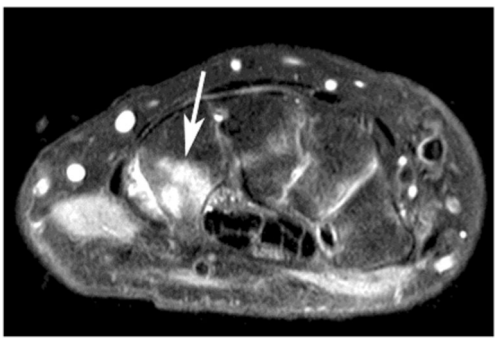

Fig. 15 Juvenile idiopathic arthritis (JIA). Axial FS PDW FSE MR image showing a BML in the hamate (*arrow*)

Fig. 16 Brodie's abscess of the distal ulna in a 7-year-old girl. **a** AP radiograph showing an irregular lytic lesion (*arrow*) with associated extensive periosteal response (*arrowheads*). **b** Coronal T1W SE MR image showing a bone abscess (*arrow*). **c** Axial FS PDW FSE MR image showing a prominent BML (*arrow*) and associated soft tissue edema (*arrowheads*)

Inflammatory arthropathy

BML is also a feature of juvenile idiopathic arthritis (JIA) (Fig. 15) [69]. Dynamic contrast-enhanced (DCE) MRI correlates well with clinical activity in JIA [70]. However, the degree of synovial enhancement is dependent upon the time between injection and imaging, being greater 10 min post-injection compared to immediately post-injection [71]. Efforts are being made to develop MRI scoring systems for both the wrist and knee in JIA [72]. BML, synovial thickening, and joint effusion are also common MRI findings in juvenile psoriatic arthritis [73].

Trauma

As with adults, carpal fractures may be radiographically occult in the pediatric population. In a study looking at pediatric carpal fractures, MRI was performed for persistent symptoms on just over 50% of cases at a mean of 17 days post-injury [74]. In 63% of these children, an occult carpal fracture was identified, most commonly involving the scaphoid, capitate and triquetrum. Simple BML was also seen in a few cases.

Infection

Hematogenous osteomyelitis is commoner in children [75]. In pediatric wrist OM, the distal radius and ulna are relatively common sites [75]. Sub-acute OM, or Brodie's abscess, is characterized by the 'penumbra sign', a rim of relative T1W

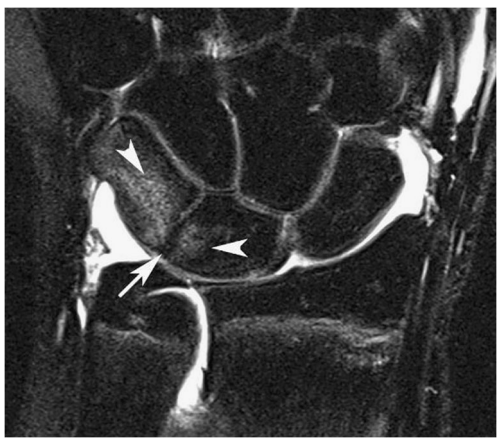

Fig. 17 Carpal coalition. Coronal STIR MR image of a 14-year-old boy who injured his wrist, showing a fibrous luno-triquetral coalition (*arrow*) with associated BML in both bones (*arrowheads*). (c/o Dr. Imran Khan)

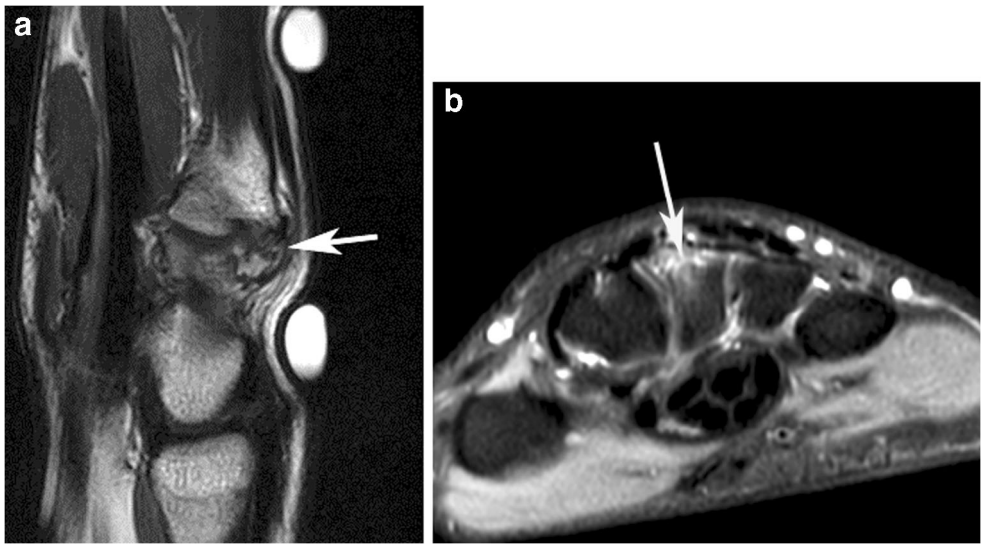

Fig. 18 Carpal boss. **a** Sagittal T2W FSE and **b** axial FS PDW FSE MR images showing a dorsal bony prominence at the junction between the capitate and 3rd metacarpal base (*arrow* in **a**) with associated BML (*arrow* in **b**)

hyperintensity around the margin of the abscess which enhances following contrast and represents the vascularized granulation tissue in the abscess wall, with adjacent intense BML (Fig. 16) [76].

Congenital

Carpal coalition refers to the fusion of two or more carpal bones, with a prevalence of 2% in the general population [77], and can be bony (synostosis), fibrous (syndesmosis) or cartilaginous (synchondrosis). The most common coalitions are the capito-hamate and luno-triquetral [77]. Carpal coalitions tend to be asymptomatic, although fibrous or cartilaginous coalitions may be associated with localized BML (Fig. 17) [78]. Other bony pseudarthroses that can result in BML in the wrist include the carpal boss, which is located at the base of the 2nd or 3rd metacarpal [79]. BML at this site correlates with pain (Fig. 18) [80].

Normal variants and imaging artefact

BMLs have been described in asymptomatic adults of varying age, notably in the scaphoid [81]. When encountered with high SI on fluid-sensitive sequences, it is important to exclude MRI artefact as a potential contributory cause. Fat-suppressed sequences are more prone to susceptibility artefact when compared with STIR. Inadequate fat suppression can be easily distinguished from pathology, as the adjacent subcutaneous fat may also be involved (Fig. 19) [82]. If the marrow hyperintensity has a linear distribution with alternating low

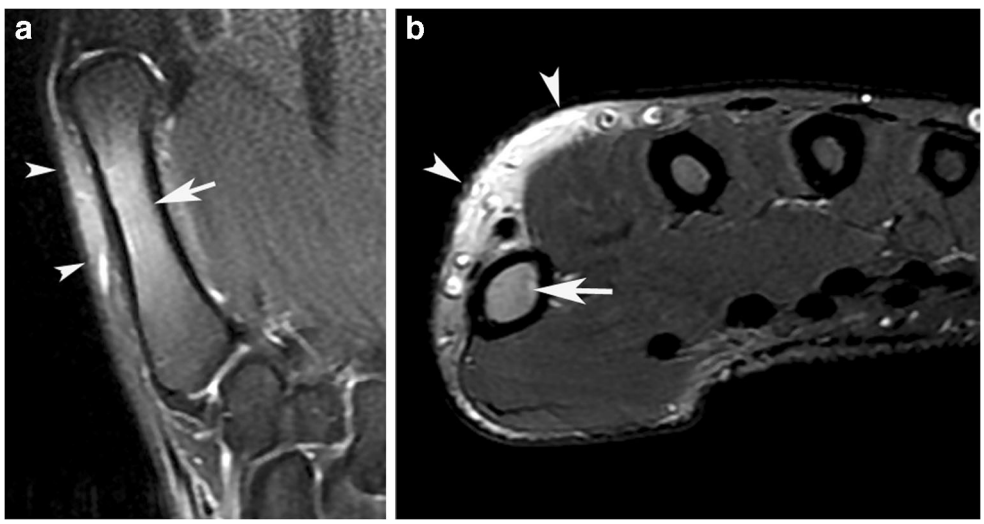

Fig. 19 MR artefact. **a** Coronal and **b** axial fat-suppressed T2W FSE MR images of a 31-year-old female showing increased marrow SI in the thumb metacarpal (*arrows*) and overlying skin (*arrowheads*) due to poor fat suppression

and bright SI in the plane of the wrist vessels, this will be due to phase-encoding artefact [82].

Conclusions

BML is a sensitive, although commonly non-specific finding with multiple etiologies. This review article highlights different patterns of wrist BML broadly categorized according to the 'surgical sieve' mnemonic method to aid in wrist MRI interpretation. Physiologic marrow changes and potential imaging artefacts have also been briefly discussed.

Compliance with ethical standards

Conflict of interest None.

Consent and ethics Not applicable.

References

1. Alam F, Schweitzer ME, Li XX, Malat J, Hussain SM. Frequency and spectrum of abnormalities in the bone marrow of the wrist: MR imaging findings. Skelet Radiol. 1999;28(6):312–7.
2. Manara M, Varenna M. A clinical overview of bone marrow oedema. Reumatismo. 2014;66(2):184–96.
3. Wilson AJ, Murphy WA, Hardy DC, Totty WG. Transient osteoporosis: transient bone marrow oedema? Radiology. 1988;167(3):757–60.
4. O'Hare A, Shortt C, Napier N, Eustace SJ. Bone marrow edema: patterns and clinical implications. Semin Musculoskelet Radiol. 2006;10(4):249–57.
5. Janowski J, Coady C, Catalano LW 3rd. Scaphoid fractures: nonunion and malunion. J Hand Surg Am. 2016;41(11):1087–92. https://doi.org/10.1016/j.jhsa.2016.08.019.
6. Klifto CS, Ramme AJ, Sapienza A, Paksima N. Scaphoid nonunions. Bull Hosp Jt Dis (2013). 2018;76(1):27–32.
7. Danger F, Wasyliw C, Varich L. Osteochondroses. Semin Musculoskelet Radiol. 2018;22(1):118–24. https://doi.org/10.1055/s-0038-1627094.
8. Murthy NS. The role of magnetic resonance imaging in scaphoid fractures. J Hand Surg Am. 2013;38(10):2047–54. https://doi.org/10.1016/j.jhsa.2013.03.055.
9. Bervian MR, Ribak S, Livani B. Scaphoid fracture nonunion: correlation of radiographic imaging, proximal fragment histologic viability evaluation and estimation of viability at surgery: diagnosis of scaphoid pseudarthrosis. Int Orthop. 2015;39(1):67–72.
10. Fox MG, Gaskin CM, Chhabra AB, Anderson MW. Assessment of scaphoid viability with MRI: a reassessment of findings on unenhanced MR images. AJR Am J Roentgenol. 2010;195(4):W281–6. https://doi.org/10.2214/AJR.09.4098.
11. Kalainov DM, Cohen MS, Hendrix RW, Sweet S, Culp RW, Osterman AL. Preiser's disease: identification of two patterns. J Hand Surg Am. 2003;28(5):767–78.
12. Schmitt R, Fröhner S, van Schoonhoven J, Lanz U, Gölles A. Idiopathic osteonecrosis of the scaphoid (Preiser's disease)—MRI gives new insights into etiology and pathology. Eur J Radiol. 2011;77(2):228–34. https://doi.org/10.1016/j.ejrad.2010.11.009.
13. Tomori Y, Motoda N, Ohashi R, Sawaizumi T, Nanno M, Takai S. Preiser disease after repeated local glucocorticoid injections: a case report. Medicine (Baltimore). 2018;97(38):e12413. https://doi.org/10.1097/MD.0000000000012413.
14. Fontaine C. Kienböck's disease. Chir Main. 2015;34(1):4–17. https://doi.org/10.1016/j.main.2014.10.149.
15. Nealey EM, Petscavage-Thomas JM, Chew FS, Allan CH, Ha AS. Radiologic guide to surgical treatment of Kienbock's disease. Curr Probl Diagn Radiol. 2018;47(2):103–9. https://doi.org/10.1067/j.cpradiol.2017.04.012.
16. Arnaiz J, Piedra T, Cerezai L, et al. Imaging of Kienbock disease. Am J Roentgenol. 2014;203:131–9.
17. Peters SJ, Degreef I, De Smet L. Avascular necrosis of the capitate: report of six cases and review of the literature. J Hand Surg Eur Vol. 2015;40(5):520–5. https://doi.org/10.1177/1753193414524876.
18. Starr AM, Wessely MA, Albastaki U, Pierre-Jerome C, Kettner NW. Bone marrow edema: pathophysiology, differential diagnosis, and imaging. Acta Radiol. 2008;49(7):771–86.
19. Honda H, McDonald JR. Current recommendations in the management of osteomyelitis of the hand and wrist. J Hand Surg Am. 2009;34(6):1135–6.
20. Hsu CY, Lu HC, Shih TT. Tuberculous infection of the wrist: MRI features. AJR Am J Roentgenol. 2004;183(3):623–8.
21. Murthy NS, Ringler MD. MR imaging of carpal fractures. Magn Reson Imaging Clin N Am. 2015;23(3):405–16. https://doi.org/10.1016/j.mric.2015.04.006.
22. Mallee WH, Wang J, Poolman RW, et al. Computed tomography versus MRI versus bone scintigraphy for clinically suspected scaphoid fractures in patients with negative plain radiographs. Cochrane Database Syst Rev. 2015;6:CD010023.
23. Cockenpot E, Lefebvre G, Demondion X, Chantelot C, Cotten A. Imaging of sports-related hand and wrist injuries: sports imaging series. Radiology. 2016;279(3):674–92. https://doi.org/10.1148/radiol.2016150995.
24. Tibrewal S, Jayakumar P, Vaidya S, Ang SC. Role of MRI in the diagnosis and management of patients with clinical scaphoid fracture. Int Orthop. 2012;36(1):107–10. https://doi.org/10.1007/s00264-011-1350-3.
25. Thavarajah D, Syed T, Shah Y, Wetherill M. Does scaphoid bone bruising lead to occult fracture? A prospective study of 50 patients. Injury. 2011;42:1303–6. https://doi.org/10.1016/j.injury.2011.02.020.
26. Mandegaran R, Gidwani S, Zavareh A. Concomitant hook of hamate fractures in patients with scaphoid fracture: more common than you might think. Skelet Radiol. 2018;47(4):505–10.
27. Becce F, Theumann N, Bollmann C, et al. Dorsal fractures of the triquetrum: MRI findings with an emphasis on dorsal carpal ligament injuries. AJR Am J Roentgenol. 2013;200(3):608–17. https://doi.org/10.2214/AJR.12.8736.
28. Van Demark RE, Van Demark RE, Helsper E. Stress fracture of the hook of the hamate: a case report. S D Med. 2015;68(4):161.
29. Bancroft LW. Wrist injuries: a comparison between high- and low-impact sports. Radiol Clin N Am. 2013;51(2):299–311. https://doi.org/10.1016/j.rcl.2012.09.017.
30. Dwek JR, Cardoso F, Chung CB. MR imaging of overuse injuries in the skeletally immature gymnast: spectrum of soft-tissue and osseous lesions in the hand and wrist. Pediatr Radiol. 2009;39(12):1310–6.
31. Maquirriain J, Ghisi JP. Stress injury of the lunate in tennis players: a case series and related biomechanical considerations. Br J Sports Med. 2007;41(11):812–5.
32. Krestan CR, Nemec U, Nemec S. Imaging of insufficiency fractures. Semin Musculoskelet Radiol. 2011;15(3):198–207.
33. Brown RR, Fliszar E, Cotten A, Trudell D, Resnick D. Extrinsic and intrinsic ligaments of the wrist: normal and pathologic anatomy

at MR arthrography with three compartmental enhancement. Radiographics. 1998;18:667–74.
34. Bateni CP, Bartolotta RJ, Richardson ML, Mulcahy H, Allan CH. Imaging key wrist ligaments: what the surgeon needs the radiologist to know. AJR Am J Roentgenol. 2013;200(5):1089–95.
35. Strauch RJ. Scapholunate advanced collapse and scaphoid nonunion advanced collapse arthritis—update on evaluation and treatment. J Hand Surg Am. 2011;36(4):729–35. https://doi.org/10.1016/j.jhsa.2011.01.018.
36. Tischler BT, Diaz LE, Murakami AM, et al. Scapholunate advanced collapse: a pictorial review. Insights Imaging. 2014;5(4):407–17. https://doi.org/10.1007/s13244-014-0337-1.
37. Taneja AK, Bredella MA, Chang CY, Joseph Simeone F, Kattapuram SV, Torriani M. Extrinsic wrist ligaments: prevalence of injury by magnetic resonance imaging and association with intrinsic ligament tears. J Comput Assist Tomogr. 2013;37(5):783–9. https://doi.org/10.1097/RCT.0b013e318298aa2a.
38. DaSilva MF, Goodman AD, Gil JA, Akelman E. Evaluation of ulnar-sided wrist pain. J Am Acad Orthop Surg. 2017;25(8):e150–6. https://doi.org/10.5435/JAAOS-D-16-00407.
39. Ersoy H, Pomeranz SJ. Palmer classification and magnetic resonance imaging findings of ulnocarpal impingement. J Surg Orthop Adv. 2015;24(4):257–62.
40. Cerezal L, del Piñal F, Abascal F, García-Valtuille R, Pereda T, Canga A. Imaging findings in ulnar-sided wrist impaction syndromes. Radiographics. 2002;22(1):105–21.
41. Reijnierse M, Helm-Mil AV, Eshed I, Schueller-Weidekamm C. Magnetic resonance imaging of rheumatoid arthritis: peripheral joints and spine. Semin Musculoskelet Radiol. 2018;22(2):127–46. https://doi.org/10.1055/s-0038-1639474.
42. Chen B, Zhang L, Guo W. Metacarpophalangeal and wrist MRI bone marrow oedema can reflect the disease activity of rheumatoid arthritis and correlate with SDAI, CDAI and DAS28. Biomed Res. 2016;27(3):616–22.
43. Woodworth TG, Morgacheva O, Pimienta OL, Troum OM, Ranganath VK, Furst DE. Examining the validity of the rheumatoid arthritis MRI score according to the OMERACT filter—a systematic literature review. Rheumatology (Oxford). 2017;56(7):1177–88.
44. Li X, Yu A, Virayavanich W, Noworolski SM, Link TM, Imboden J. Quantitative characterization of bone marrow edema pattern in rheumatoid arthritis using 3 Tesla MRI. J Magn Reson Imaging. 2012;35(1):211–7.
45. Nieuwenhuis WP, van Steenbergen HW, Stomp W, et al. The course of bone marrow edema in early undifferentiated arthritis and rheumatoid arthritis: a longitudinal magnetic resonance imaging study at bone level. Arthritis Rheumatol. 2016;68(5):1080–8.
46. Fujimori M, Nakamura S, Hasegawa K, et al. Cartilage quantification using contrast-enhanced MRI in the wrist of rheumatoid arthritis: cartilage loss is associated with bone marrow edema. Br J Radiol. 2017;90(1077):20170167. https://doi.org/10.1259/bjr.20170167.
47. McQueen F, Lassere M, Edmonds J, Conaghan P, Peterfy C, Bird P, et al. OMERACT rheumatoid arthritis magnetic resonance imaging studies. Summary of OMERACT 6 MR imaging module. J Rheumatol. 2003;30(6):1387–92.
48. Narváez J, Narváez JA, de Albert M, Gómez-Vaquero C, Nolla JM. Can MRI of the hand and wrist differentiate between rheumatoid arthritis and psoriatic arthritis in the early stages of the disease? Semin Arthritis Rheum. 2012;42(3):234–45.
49. Tani C, D'Aniello D, Possemato N, et al. MRI pattern of arthritis in systemic lupus erythematosus: a comparative study with rheumatoid arthritis and healthy subjects. Skelet Radiol. 2015;44(2):261–6.
50. Barnes CL, Helms CA. MRI of gout: a pictorial review. Int J Clin Rheumatol. 2012;7(3):281–5.
51. Emad Y, Ragab Y, El-Naggar A, et al. Gadolinium-enhanced MRI features of acute gouty arthritis on top of chronic gouty involvement in different joints. Clin Rheumatol. 2015;34(11):1939–47.
52. Poh YJ, Dalbeth N, Doyle A, McQueen FM. Magnetic resonance imaging bone edema is not a major feature of gout unless there is concomitant osteomyelitis: 10-year findings from a high-prevalence population. J Rheumatol. 2011;38(11):2475–81.
53. Tomlinson RE, Silva MJ. Skeletal blood flow in bone repair and maintenance. Bone Research. 2013;4:311–22.
54. Murray PM, Berger RA, Inwards CY. Primary neoplasms of the carpal bones. J Hand Surg Am. 1999;24(5):1008–13.
55. Jafari D, Shariatzade H, Mazhar FN, Abbasgholizadeh B, Dashtebozorgh A. Osteoid osteoma of the hand and wrist: a report of 25 cases. Med J Islam Repub Iran. 2013;27(2):62–6.
56. Kaim AH, Hugli R, Bonel HM, Jundt G. Chondroblastoma and clear cell chondrosarcoma: radiological and MRI characteristics with histopathological correlation. Skelet Radiol. 2002;31(2):88–95.
57. Davila JA, Amrami KK, Sundaram M, Adkins MC, Unni KK. Chondroblastoma of the hands and feet. Skelet Radiol. 2004;33(10):582–7.
58. Schurmann M, Zaspel J, Lohr P, et al. Imaging in early post-traumatic complex regional pain syndrome: a comparison of diagnostic methods. Clin J Pain. 2007;23(5):449–57.
59. de Abreu MR, Wesselly M, Chung CB, Resnick D. Bone marrow MR imaging findings in disuse osteoporosis. Skelet Radiol. 2011;40(5):571–5. https://doi.org/10.1007/s00256-010-1042-x.
60. Rios AM, Rosenberg ZS, Bencardino JT, Rodrigo SP, Theran SG. Bone marrow oedema patterns in the ankle and hindfoot: distinguishing MRI features. Am J Roentgenol. 2011;197:W720–9. https://doi.org/10.2214/AJR.10.5880.
61. Feydy A, Pluot E, Guerini H, Drapé JL. Osteoarthritis of the wrist and hand, and spine. Radiol Clin N Am. 2009;47(4):723–59. https://doi.org/10.1016/j.rcl.2009.06.004.
62. Laulan J, Marteau E, Bacle G. Wrist osteoarthritis. Orthop Traumatol Surg Res. 2015;101(1 Suppl):S1–9. https://doi.org/10.1016/j.otsr.2014.06.025.
63. Wollstein R, Clavijo J, Gilula LA. Osteoarthritis of the wrist STT joint and radiocarpal joint. Arthritis. 2012;2012:242159. https://doi.org/10.1155/2012/242159.
64. Carrino JA, Blum J, Parellada JA, Schweitzer ME, Morrison WB. MRI of bone marrow edema-like signal in the pathogenesis of subchondral cysts. Osteoarthr Cartil. 2006;14(10):1081–5.
65. Gornitzky AL, Lin IC, Carrigan RB. The diagnostic utility and clinical implications of wrist MRI in the pediatric population. Hand (N Y). 2018;13(2):143–9. https://doi.org/10.1177/1558944717695752.
66. Taylor KW, Moore MM, Brian J, Methratta S, Bernard S. Wrist MR imaging in children: effect on clinical diagnosis and management. Clin Imaging. 2017;44:61–5. https://doi.org/10.1016/j.clinimag.2017.04.001.
67. Shabshin N, Schweitzer ME. Age dependent T2 changes of bone marrow in pediatric wrist MRI. Skelet Radiol. 2009;38(12):1163–8. https://doi.org/10.1007/s00256-009-0752-4.
68. Avenarius DFM, Ording Müller LS, Rosendahl K. Joint fluid, bone marrow edema like changes, and ganglion cysts in the pediatric wrist: features that may mimic pathologic abnormalities-follow-up of a healthy cohort. Am J Roentgenol. 2017;208(6):1352–7.
69. Tanturri de Horatio L, Damasio MB, Barbuti D, et al. MRI assessment of bone marrow in children with juvenile idiopathic arthritis: intra- and inter-observer variability. Pediatr Radiol. 2012;42(6):714–20.
70. Nusman CM, Lavini C, Hemke R, et al. Dynamic contrast-enhanced magnetic resonance imaging of the wrist in children with juvenile idiopathic arthritis. Pediatr Radiol. 2017;47(2):205–13. https://doi.org/10.1007/s00247-016-3736-2.

71. Rieter JF, de Horatio LT, Nusman CM, et al. The many shades of enhancement: timing of post-gadolinium images strongly influences the scoring of juvenile idiopathic arthritis wrist involvement on MRI. Pediatr Radiol. 2016;46(11):1562–7. https://doi.org/10.1007/s00247-016-3657-0.
72. Nusman CM, Ording Muller LS, Hemke R, et al. Current status of efforts on standardizing magnetic resonance imaging of juvenile idiopathic arthritis: report from the OMERACT MRI in JIA working group and health-e-child. J Rheumatol. 2016;43(1):239–44. https://doi.org/10.3899/jrheum.141276.
73. Lee EY, Sundel RP, Kim S, Zurakowski D, Kleinman PK. MRI findings of juvenile psoriatic arthritis. Skelet Radiol. 2008;37(11):987–96. https://doi.org/10.1007/s00256-008-0537-1.
74. Eckert K, Tröbs RB, Schweiger B, Liedgens P, Radeloff E, Ackermann O. [Diagnostically approach to pediatric carpal fractures: a retrospective analysis]. [Article in German]. Z Orthop Unfall. 2016;154(1):43–9. https://doi.org/10.1055/s-0035-1558078.
75. Fitoussi F, Litzelmann E, Ilharreborde B, Morel E, Mazda K, Penneçot GF. Hematogenous osteomyelitis of the wrist in children. J Pediatr Orthop. 2007;27(7):810–3.
76. Kornaat PR, Camerlinck M, Vanhoenacker FM, De Praeter G, Kroon HM. Brodie's abscess revisited. JBR-BTR. 2010;93(2):81–6.
77. Resnik CS, Grizzard JD, Simmons BP, Yaghmai I. Incomplete carpal coalition. AJR. 1986;147:301–4.
78. Simmons BP, McKenzie WD. Symptomatic carpal coalition. J Hand Surg Am. 1985;10(2):190–3.
79. Porrino J, Maloney E, Chew FS. Current concepts of the carpal boss: pathophysiology, symptoms, clinical or imaging diagnosis, and management. Curr Probl Diagn Radiol. 2015;44(5):462–8. https://doi.org/10.1067/j.cpradiol.2015.02.008.
80. Mespreuve M, De Smet L, De Cuyper K, Waked K, Vanhoenacker F. MRI diagnosis of carpal boss and comparison with radiography. Acta Radiol. 2017;58(10):1245–51.
81. Mangnus L, van Steenbergen HW, Reijnierse M, van der Helm-van Mil AH. Magnetic resonance imaging-detected features of inflammation and erosions in symptom-free persons from the general population. Arthritis Rheumatol. 2016;68(11):2593–602.
82. Morelli JN, Runge VM, Attenberger U, et al. An image-based approach to understanding the physics of MR artifacts. Radiographics. 2011;31(3):849–66.